A new analytical solution for assessing climate change impacts on subsurface temperature

This is a post-print of an article published in *Hydrological Processes* in 2014. For publishers version email: barret.kurylyk@dal.ca or visit http://onlinelibrary.wiley.com/doi/10.1002/hyp.9861/abstract

Authors
Barret L. Kurylyk and Kerry T. B. MacQuarrie, University of New Brunswick, Department of Civil Engineering and Canadian Rivers Institute, Fredericton, New Brunswick, Canada.

Abstract

Groundwater temperature is an important water quality parameter that affects species distributions in subsurface and surface environments. To investigate the response of subsurface temperature to atmospheric climate change, an analytical solution is derived for a one-dimensional, transient conduction-advection equation and verified with numerical methods using the finite element code SUTRA. The solution can be applied to forward model the impact of climate change on subsurface temperature profiles, or applied in an inverse manner to produce a surface temperature history from measured borehole profiles. The initial conditions are represented using superimposed linear and exponential functions, and the boundary condition is given as an exponential function. This solution expands on a classic solution in which the initial and boundary conditions were restricted to linear functions. The exponential functions allow more flexibility in matching climate model projections (boundary conditions) and measured temperature-depth profiles (initial conditions). For example, measured borehole temperature data from the Sendai Plain and Tokyo, Japan were used to demonstrate the improved accuracy of the exponential function for replicating temperature-depth profiles. Also, the improved accuracy of the exponential boundary condition was demonstrated using air temperature anomaly data from the Intergovernmental Panel on Climate Change. These air temperature anomalies were then used to forward model the subsurface effect of surficial thermal perturbations. The simulation results indicate that recharge can accelerate shallow subsurface warming, while upward groundwater discharge can enhance deeper subsurface warming. Additionally, the simulation results demonstrate that future groundwater temperatures obtained from the proposed analytical solution can deviate significantly from those produced with the classic solution.

Keywords: groundwater temperature, subsurface warming, thermal regime, climate change, soil temperature

1. Introduction

1.1. Importance of groundwater temperature

Groundwater temperature is less variable than surface water temperature, thus groundwater discharge can stabilize river temperatures during winter and summer months (Hayashi and Rosenberry, 2002; Caissie, 2006; Webb *et al*., 2008). Discrete cold-water plumes formed by groundwater-surface water interactions have also been shown to provide critical thermal relief for cold-water fish during high-temperature events (Cunjak *et al.*, 2005; Breau *et al.*, 2011; Torgersen *et al.*, 2012). In a warming climate, the ecology of riverine systems may become increasingly dependent on groundwater discharge. Groundwater temperature can also affect subsurface biogeochemical processes and influence the distribution of unicellular and multicellular microorganisms in the subsurface and in surface water at points of groundwater discharge (Rike *et al*., 2008; Andrushchyshyn *et al*., 2009; Green *et al*., 2011; Roy *et al*., 2011; Sharma *et al*., 2012). Thus groundwater temperature can affect species richness in subsurface and riverine ecosystems and thereby impact groundwater and surface water quality. Because aquifer and river thermal regimes are interrelated, there is a need for further studies examining the effect of climate change on groundwater temperature. For example, Mayer (2012) has recently noted: 'The future warming of shallow groundwater temperature…could affect stream temperatures…One challenge to assessing this is that most studies of climate change impacts to groundwater have focused on changes to recharge and sub-surface flow rather than effects to groundwater temperature.'

Recent climate change effects on surface and shallow subsurface temperature have already been observed (e.g., Qian *et al*., 2011), and climate model projections for the coming decades indicate that significant warming will occur on a regional and global scale (Solomon *et al*., 2007). Groundwater temperature will respond to a warming climate as rising ground surface temperature trends will be propagated through the subsurface (Taylor and Stefan, 2009); however, very little research has been conducted on the impact of future climate change on groundwater temperature.

1.2. History and limitations of conduction heat transport mathematics

The subsurface thermal regime is driven by energy and water exchanges at the ground surface and the geothermal heat flux from the Earth's interior. Ground surface temperature signals are transported and retained in the subsurface, but the amplitude of the temperature variation (e.g., daily or seasonal temperature fluctuations) exponentially attenuates with depth due to the process of heat diffusion and the ability of the soil and water to retain heat (Carslaw and Jaeger, 1959; Lunardini, 1981; Williams and Smith, 1989). High frequency ground surface temperature signals (e.g., monthly) are only retained at shallow depths, but lower frequency signals (e.g., decadal climate change) may be retained at great depths (Lesperance *et al*., 2010).

Early subsurface heat transport analyses were predicated on the assumption that conduction was the dominant form of heat transport. Birch (1948) proposed that the distribution of subsurface temperature could be used to infer past climatic conditions by analyzing a transient form of the conduction equation. His theory has since been expanded to reproduce paleoclimates by inverting temperature-depth profiles (e.g., Lachenbruch and Marshall, 1986; Mareschal and Beltrami, 1992; Beltrami *et al*., 1995; Harris and Chapman, 1997; Pollack *et al*., 1998; Lesperance *et al*., 2010). These results have been used to assess the validity of global climate model (GCM) simulations of past climates. Conduction-based analytical solutions have also been used to forward model the effects of past climate change by using measured or GCM-simulated air temperature history to perturb an assumed initial geothermal profile (Beltrami *et al*., 2005; González-Rouco *et al*., 2006). Other solutions to the transient heat conduction equation under a variety of initial and boundary conditions have been compiled by Carslaw and Jaeger (1959), Özışık (1968), and Crank (1980).

Conduction-based techniques for paleoclimate inversion may be invalid in regions of significant groundwater flow because the subsurface thermal signature used to infer surficial climate change may have resulted from advective heat transport (Lewis and Wang, 1992; Kukkonen *et al*., 1994; Bodri and Cermak, 2005; Ferguson *et al*., 2006). For example, both ground surface temperature increases and downward groundwater flow can induce a concave upward temperature distribution (Figure 1). Bodri and Cermak (2005) observed that the effects of advection were discernible in their simulated one-dimensional temperature profiles when Darcy flux exceeded 1×10^{-9} m·s^{-1} (0.032 m·yr^{-1}). Thus, the assumption that conduction is the only significant form of heat transport may be invalid for regions where water or vapor transport are significant (Woodbury and Smith, 1985; van der Kamp and Bachu, 1989; Hinkel and Outcalt, 1993; Kane *et al*., 2001; McKenzie and Voss, 2013).

1.3. Groundwater temperature as a tracer for groundwater velocity

Suzuki (1960) first proposed that temperature-depth profiles could be used to estimate rates of vertical groundwater flow by solving the following one-dimensional conduction-advection equation for semi-infinite media:

$$\lambda \frac{\partial^2 T}{\partial z^2} - q c_w \rho_w \frac{\partial T}{\partial z} = c\rho \frac{\partial T}{\partial t} \qquad (1)$$

where λ is the thermal conductivity of the medium (M·L·t^{-3}·T^{-1}), T is temperature, z is depth below ground surface (L), q is the vertical Darcy flux (positive downwards, L·t^{-1}), $c_w\rho_w$ is the volumetric heat capacity of water (M·L^{-1}·t^{-2}·T^{-1}), $c\rho$ is the volumetric heat capacity of the medium (M·L^{-1}·t^{-2}·T^{-1}), and t is time. Suzuki (1960) solved this equation by applying a periodic first-type boundary condition to represent the annual cycle of ground surface temperature. Stallman (1963; 1965) later provided a more detailed derivation of the governing equation (1) and the solution for determining groundwater velocity based on the

subsurface temperature distribution. The methods for using groundwater temperature to estimate groundwater velocity have been comprehensively reviewed by Anderson (2005) and Saar (2011).

1.4. Combined effects of groundwater flow and ground surface temperature rise

A temperature-depth profile that is assumed to have been induced by vertical groundwater flow may have actually arisen from long-term climate change (Ferguson and Woodbury, 2005; Reiter, 2005); this is the converse of the problem facing paleoclimatologists. To address this issue, Taniguchi *et al*. (1999) modified an analytical solution by Carslaw and Jaeger (1959, p. 388) to account for both surface temperature changes and vertical groundwater flow. The governing equation is of the same form as equation (1); the initial conditions, boundary condition and solution are given below:

$$\text{Initial Conditions: } T\left(z, t=0\right) = T_0 + az$$

$$\text{Boundary Condition: } T\left(z=0, t\right) = T_0 + \varphi t$$

$$\begin{aligned} \text{Solution}: T\left(z,t\right) &= T_0 + a\left(z - vt\right) + \frac{1}{2v}\left(\varphi + va\right)\times \\ &\left[\left(vt - z\right)\times erfc\left(\frac{z - Vt}{2\sqrt{Dt}}\right) + \left(vt + z\right)\exp\left(\frac{vz}{\alpha}\right)erfc\left(\frac{z + vt}{2\sqrt{Dt}}\right)\right] \end{aligned} \tag{2}$$

where T_0 is the initial surface temperature, a is the geothermal gradient ($T\cdot L^{-1}$), *erfc* is the complementary error function, φ is the slope of the linear ground surface temperature rise ($T\cdot t^{-1}$), D is the thermal diffusivity of the medium = $\lambda(c\rho)^{-1}$ ($L^2\cdot t^{-1}$), and $v = qc_w\rho_w(c\rho)^{-1}$ ($L\cdot t^{-1}$).

Taniguchi *et al*. (1999) proposed that this analytical solution could be used to determine groundwater fluxes in regions of measured surface temperature rise due to urbanization or climate change; conversely, if the groundwater flux was known, the solution could be inverted to reproduce a linear ground surface temperature history from borehole temperature data (Miyakoshi *et al*., 2003; Taniguchi *et al*., 2003; Uchida *et* al., 2003; Taniguchi and Uemura, 2005; Uchida and Hayashi, 2005; Taniguchi, 2006; Taniguchi *et al*., 2009). This solution has also been recently applied to forward model future groundwater temperature based on downscaled climate change projections for the Sendai Plain, Japan (Gunawardhana *et al*., 2011; Gunawardhana and Kazama, 2011).

1.5. Improved boundary and initial conditions using exponential functions

GCMs simulate atmospheric, surficial, and oceanic processes to project future climate regimes due to increased atmospheric greenhouse gas concentrations (Solomon *et al*., 2007). The Intergovernmental Panel on Climate Change (IPCC, 2007) compiled multi-model

averages for global air temperature anomalies for 2000-2099 from 24 GCM's driven by emission scenarios B1, A1B and A2. The multi-model A2 emission scenario results are characterized by significant concavity that may be better represented by boundary conditions containing an exponential function, rather than the linear boundary conditions available in existing conduction-advection solutions. Some previous solutions to the transient conduction equation have employed a series of superimposed step functions as the surface boundary condition (e.g., Beltrami *et al*., 2005). This boundary condition can mimic surface temperature history or projections better than a linear function, but these solutions have limited applicability for simulating subsurface temperature evolution when advection is significant.

Although we utilized air temperature anomalies to form our boundary condition, we acknowledge that the ground surface temperature, not the air temperature, drives the subsurface thermal regime (Lunardini, 1981). It is well-established that high frequency (e.g., daily or seasonal) air temperatures and ground surface temperature variations are decoupled due to snow cover insulating effects, latent heat arising from freeze/thaw phase changes, shading from vegetation, and other factors (e.g., Beltrami and Kellman, 2003; Beltrami *et al*., 2005; Zhang, 2005; Smerdon *et al*., 2006). This short term decoupling does not necessitate a decoupling between low frequency (e.g., decadal) variations in air temperature and ground surface temperature, and there remains an ongoing debate regarding the coupling of air temperature and ground surface temperature anomalies in past or projected long-term climate change (e.g., Mann and Schmidt, 2003; Smerdon *et al*., 2004; Beltrami *et al*., 2005; Pollack *et al*., 2005; González-Rouco *et al*., 2006; Smerdon *et al*., 2006; Stieglitz and Smerdon, 2007). It is possible that the significant rate of climate change projected for the coming decades may reduce the average length of the snow-covered period and the mean annual snowpack depth at some latitudes. This would reduce the mean annual thermal conductivity between the lower atmosphere and the ground surface and could result in differences between projected changes in decadal air temperature and ground surface temperature trends (Mellander *et al*., 2007; Kurylyk *et al*., 2013). However, following the approach of others listed above, we assume that long-term ground surface temperature changes will closely follow air temperature changes.

Measured temperature-depth profiles are also typically nonlinear. This is particularly noticeable in the shallow subsurface because of the effects of vertical groundwater fluxes or recent warming due to climate change or urbanization (Mareschal and Beltrami, 1992; Kukkonen *et al*., 1994; Ferguson and Woodbury, 2004; 2005; 2007). The present borehole temperature profile represents the initial conditions for forward modeling the subsurface thermal response to climate change, thus initial conditions functions should be capable of matching non-linear temperature profiles.

1.6. Research objectives

The intent of this contribution is to address the limitations associated with the initial and boundary conditions employed in the analytical solution developed by Carslaw and Jaeger (1959) and modified by Taniguchi *et al.* (1999). Our first objective is to demonstrate that exponential functions, which are still amenable to analytical solutions, are better representations for surface boundary conditions and initial temperature-depth profiles. Our second objective is to do develop an analytical solution for which exponential terms are included in both the boundary and initial conditions and to apply this solution in several illustrative examples.

Although numerical solution methods can be employed to simulate subsurface temperature evolution, in some cases analytical solutions offer important advantages. Javandel *et al*. (1984) noted four advantages that are relevant to the current topic: (1) analytical methods are more efficient than numerical methods when the system is poorly defined or uncertain, (2) analytical methods are more economical (computationally) than numerical methods, (3) analytical methods are useful for initial estimations, and (4) analytical methods remove the need for experienced modelers or complex numerical codes. In addition to these advantages, analytical methods can allow the user to quickly simulate the effect of varying the governing equation parameters (e.g., soil thermal properties or groundwater velocity) and the initial and boundary conditions. Additionally, analytical solutions are more stable than numerical methods and are not subject to the spatiotemporal discretization problems that may arise when employing numerical methods.

2. Methods

2.1. Development of exponential initial and boundary conditions

As previously discussed, the surface temperature projections produced by GCMs for some emission scenarios may be more appropriately simulated with an exponential Dirichlet boundary condition (3) rather than a linear surface boundary condition (2):

$$T(z=0,t) = T_1 + b\exp(ct) \tag{3}$$

where T_1 (T), b (T), and c (t^{-1}) are fitting parameters. The boundary conditions in equation (2) and equation (3) indicate that T_0 should equal T_1+b for both boundary conditions to have the same value at t =0. The ability of equation (3) to reproduce the surface temperature trends will be demonstrated in the results.

Also, existing temperature-depth profiles may be better represented with the superposition of exponential and linear functions (4), rather than with a simple geothermal gradient (2):

$$T(z, t=0) = T_i + a\,z + \delta \exp(dz) \tag{4}$$

where T_i is a fitting parameter for the initial conditions (T), a is the general geothermal gradient ($T \cdot L^{-1}$), and δ (T) and d (L^{-1}) are fitting parameters to account for recent surface temperature changes or vertical groundwater flow. The superposition of linear and exponential functions to form the initial conditions shall hereafter be referred to as the 'exponential initial conditions'. Equation (4) is flexible and capable of producing initial conditions that mimic a variety of measured temperature-depth profiles. If the d term is negative, the third term in equation (4) exponentially decays with depth and reproduces the shallow thermal signature seen in the profiles given in Figure 1 arising from surficial warming/recharge ($+\delta$ for concave upwards) or surficial cooling/discharge ($-\delta$ for convex upwards). The ability of equation (4) to reproduce existing temperature-depth profiles will also be demonstrated in the results.

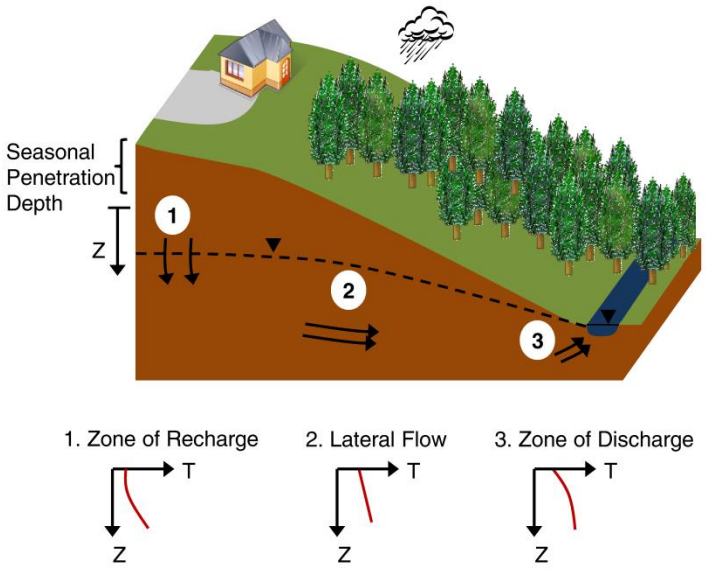

Figure 1: Temperature depth profiles for a stable climate as a function of the groundwater flow direction. Below the seasonal penetration depth, temperature-depth profiles are concave upward in groundwater recharge areas (vertical downward flow), linear in lateral flow regions (with no horizontal thermal gradient), and convex upward in discharge areas (vertical upward flow) (after, Taniguchi *et al.*, 1999; Anderson, 2005; Saar, 2011)

2.2. Development of the modified analytical solution

Equation (1) was manipulated and expressed in the standard form employed by Carslaw and Jaeger (1959):

$$D\frac{\partial^2 T}{\partial z^2} - v\frac{\partial T}{\partial z} = \frac{\partial T}{\partial t} \tag{5}$$

where D is the thermal diffusivity of the medium $\lambda(c\rho)^{-1}$ ($L^2 \cdot t^{-1}$), and $v = qc_w\rho_w(c\rho)^{-1}$ ($L \cdot t^{-1}$). The initial and boundary conditions were taken as equations (4) and (3), respectively. Our formulation for thermal conductivity/diffusivity ignores the effects of hydrodynamic dispersion, although several researchers have suggested alternative formulations that account for these effects (Molina-Giraldo *et al.*, 2011; Sauty *et al.*, 1982; Ferguson, 2007).

Typically, a partial differential equation (PDE) of this form would be first reduced to a pure diffusion equation by means of a transform of the independent variables z and t (Farlow, 1982) or the dependent variable T (Ogata and Banks, 1961). However, these techniques tend to cause the boundary condition (3) to become overly complex or spatially transferred so that it is no longer a true boundary condition. In this case, a more appropriate technique is to first reduce the PDE to an ordinary differential equation by means of the Laplace integral transform (Farlow, 1982; Trim, 1990). The subsidiary equation for this governing equation and the associated initial conditions is then:

$$D\frac{\partial^2 \overline{T}}{\partial z^2} - v\frac{\partial \overline{T}}{\partial z} - p\overline{T} = -T_i - a\,z - \delta\exp(dz) \tag{6}$$

The boundary condition (3) was used to find the solution to the subsidiary equation according to the method of undetermined coefficients (Zill, 2005):

$$\begin{aligned}\overline{T} = &\left(\frac{a\,z}{p} + \frac{T_i}{p} - \frac{va}{p^2} + \frac{\delta}{-Dd^2 + vd + p}\exp(dz)\right) + \exp\left(\frac{vz}{2D}\right)\times \\ &\left(\frac{T_1 - T_i}{p} + \frac{va}{p^2} + \frac{b}{p-c} - \frac{\delta}{(-Dd^2 + vd + p)}\right)\exp\left\{-z\sqrt{\frac{v^2}{4D^2} + \frac{p}{D}}\right\}\end{aligned} \tag{7}$$

where $\overline{T}(z, p)$ is the Laplace transform of the temperature $T(z, t)$, and p is the Laplace transform of t or the time expressed in the frequency domain. By first employing the shift theorem (Trim, 1990), then applying appropriate tabulated inverse Laplace transforms (Carslaw and Jaeger, 1959; Roberts and Kaufman, 1966), and finally making the appropriate simplifications, the following solution was obtained (see supplementary material for full derivation):

$$T = az + T_i - vat + \delta \exp\left(Dd^2t + dz - vdt\right) + \frac{(T_1 - T_i)}{2}\left\{\begin{array}{l}\operatorname{erfc}\left(\frac{z}{2\sqrt{Dt}} - \frac{v}{2}\sqrt{\frac{t}{D}}\right) \\ + \exp\left(\frac{vz}{D}\right)\operatorname{erfc}\left(\frac{z}{2\sqrt{Dt}} + \frac{v}{2}\sqrt{\frac{t}{D}}\right)\end{array}\right\}$$

$$+ \frac{va}{2}\left\{\left(t - \frac{z}{v}\right)\operatorname{erfc}\left[\frac{z}{2\sqrt{Dt}} - \frac{v}{2}\sqrt{\frac{t}{D}}\right] + \left(t + \frac{z}{v}\right) \times \exp\left(\frac{vz}{D}\right)\operatorname{erfc}\left[\frac{z}{2\sqrt{Dt}} + \frac{v}{2}\sqrt{\frac{t}{D}}\right]\right\}$$

$$+ \frac{b}{2}\exp\left\{\frac{vz}{2D} + ct\right\}\left\{\begin{array}{l}\exp\left(-z\sqrt{v^2/4D^2 + c/D}\right)\operatorname{erfc}\left(\frac{z}{2\sqrt{Dt}} - \sqrt{\left(\frac{v^2}{4D} + c\right)t}\right) \\ + \exp\left(z\sqrt{v^2/4D^2 + c/D}\right)\operatorname{erfc}\left(\frac{z}{2\sqrt{Dt}} + \sqrt{\left(\frac{v^2}{4D} + c\right)t}\right)\end{array}\right\}$$

$$- \frac{\delta}{2}\exp\left\{\left(\frac{vz}{2Dt} + Dd^2 - vd\right)t\right\}\left\{\begin{array}{l}\exp\left(-z\sqrt{v^2/4D^2 + d^2 - vd/D}\right)\operatorname{erfc}\left(\frac{z}{2\sqrt{Dt}} - \sqrt{\left(\frac{v^2}{4D} + Dd^2 - vd\right)t}\right) \\ + \exp\left(z\sqrt{v^2/4D^2 + d^2 - vd/D}\right)\operatorname{erfc}\left(\frac{z}{2\sqrt{Dt}} + \sqrt{\left(\frac{v^2}{4D} + Dd^2 - vd\right)t}\right)\end{array}\right\} \quad (8)$$

If desired, equation (8) can be solved for an initial linear temperature-depth profile by setting the δ term in equations (4) and (8) to zero.

This solution can be evaluated in a spreadsheet; however, the product term involving the exponential function and the complementary error function can be problematic. Warrick (2003) gives the following approximation that was used to evaluate equation (8):

$$\exp(x) \times \operatorname{erfc}(y) = if\left[y < 3, \exp(x) \times \operatorname{erfc}(y), \frac{\exp\left(x - y^2\right)}{\pi^{0.5} y} \times \left(1 - \frac{0.5}{y^2} + \frac{0.75}{y^4}\right)\right] \quad (9)$$

2.3. Verification of the analytical solutions with numerical methods

Equation (8) was verified by comparisons to simulations performed within the groundwater flow and heat transport model SUTRA (Voss and Provost, 2010). SUTRA is a robust finite element model that accommodates variably saturated, multi-dimensional groundwater flow and heat transport. For the present study, the initial and boundary conditions and other parameters in the model were set so that the simulations were performed for one-dimensional flow and heat transport, fully saturated conditions, and spatiotemporally-constant groundwater velocity. In this case, the SUTRA governing equations reduce to equation (1). Figure 2 shows the simplified physical scenario and numerical modeling setup.

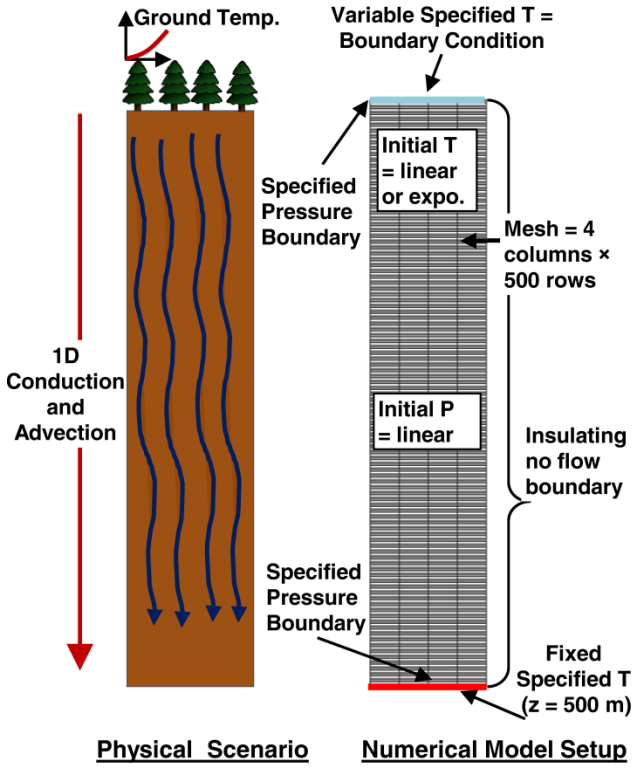

Figure 2: The assumed physical scenario and the numerical model domain used for Sutra. Appropriate initial and boundary conditions were imposed in Sutra to constrain the heat and fluid flow to the vertical dimension.

3. Results

3.1. Assessment of the exponential boundary condition

Two synthetic curves were generated to represent the IPCC (2007) projected temperature anomalies for each emission scenario for 2000-2099. The first was generated using equation (3) with the fitting parameters optimized to minimize the root-mean-square-error (RMSE) between the synthetic data and the projected data from the GCM ensemble. The second function connected the IPCC initial and final temperature anomalies for 2000-2099 using a linear boundary condition (boundary condition, equation 2) (e.g., Gunawardhana *et al*., 2011; Gunawardhana and Kazama, 2011). These curves are shown in Figure 3. It is evident that, particularly for the higher emission scenario A2, the exponential and linear curves deviate significantly from each other at mid-century (maximum difference ~0.5°C). The RMSE between each curve and the associated IPCC GCM ensemble indicated that the exponential function (RMSE = 0.032, 0.053, and 0.039 for the B1, A1B, and A2 IPCC data, respectively) provided a better fit to the climate projections than did the linear function (RMSE = 0.115, 0.081, and 0.346 for the B1, A1B, and A2 data, respectively).

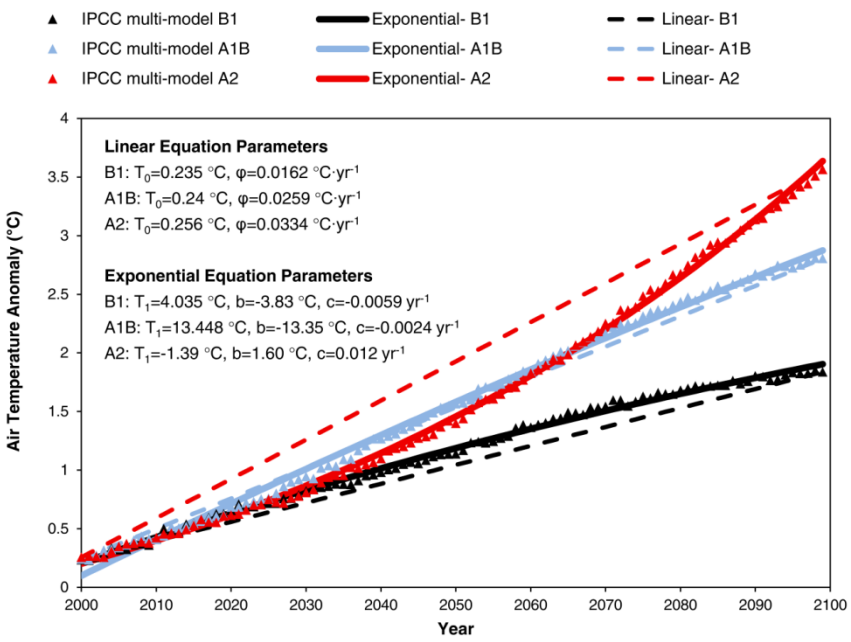

Figure 3: IPCC multi-model, globally averaged air temperature anomaly for 2000-2099 relative to 1980-1999 for emission scenarios B1, A1B, and A2 (data from, IPCC, 2007) and the linear (boundary condition, equation 2) and exponential (equation 3) functions generated to match the projections. The equation parameters are indicated.

Table 1: Fitting parameters for each curve shown in Figure 4 and the associated RMSE and R values for (a) the Sendai Plain and (b) Tokyo

Curves	**Fitting Parameters**						**Fit to Data**	
Description	T_0 (°C)	a (°C·m^{-1})	T_i (°C)	a (°C m^{-1})	δ (°C)	d (m^{-1})	RMSE	R
(A). Sendai Plain Data								
Well 1-Linear	13.261	0.0309					0.0965	0.9790
Well 4-Linear	13.501	0.0128					0.0817	0.9080
Well 5-Linear	14.095	0.0259					0.1921	0.9237
Well 1-Expo			7.804	-0.0596	5.889	0.01054	0.0141	0.9996
Well 4-Expo			7.0197	-0.0802	6.856	0.00977	0.0121	0.9981
Well 5-Expo			7.5245	0.0949	7.5656	-0.0185	0.0607	0.9926
(B). Tokyo Data								
Well 1-Linear	15.382	0.0137					0.3270	0.9117
Well 74-Linear	16.328	0.0214					0.2595	0.9542
Well 1-Expo			-2.886	0.0701	19.513	-0.0046	0.0257	0.9994
Well 74-Expo			15.603	0.0283	3.352	-0.0670	0.0440	0.9987

3.2. Assessment of the exponential initial conditions

To demonstrate the ability of equation (4) to match temperature-depth profiles, measured subsurface temperature data were obtained for the Sendai Plain, Japan (Gunawardhana, pers. communication, 2012) and for Tokyo, Japan (Taniguchi, pers. communication, 2012). Figure 4 shows the temperature data for depths below the seasonal penetration depth (> 10 m). A linear function (initial conditions, equation 2) and an exponential function (equation 4) were used to match the measured profiles by minimizing the RMSE between the measured and calculated temperature-depth profiles (Figure 4). The fitting parameters are indicated in Table 1 along with the associated RMSE and correlation coefficient (R values). It is evident that the exponential function does a far superior job of replicating the measured profile in all five instances.

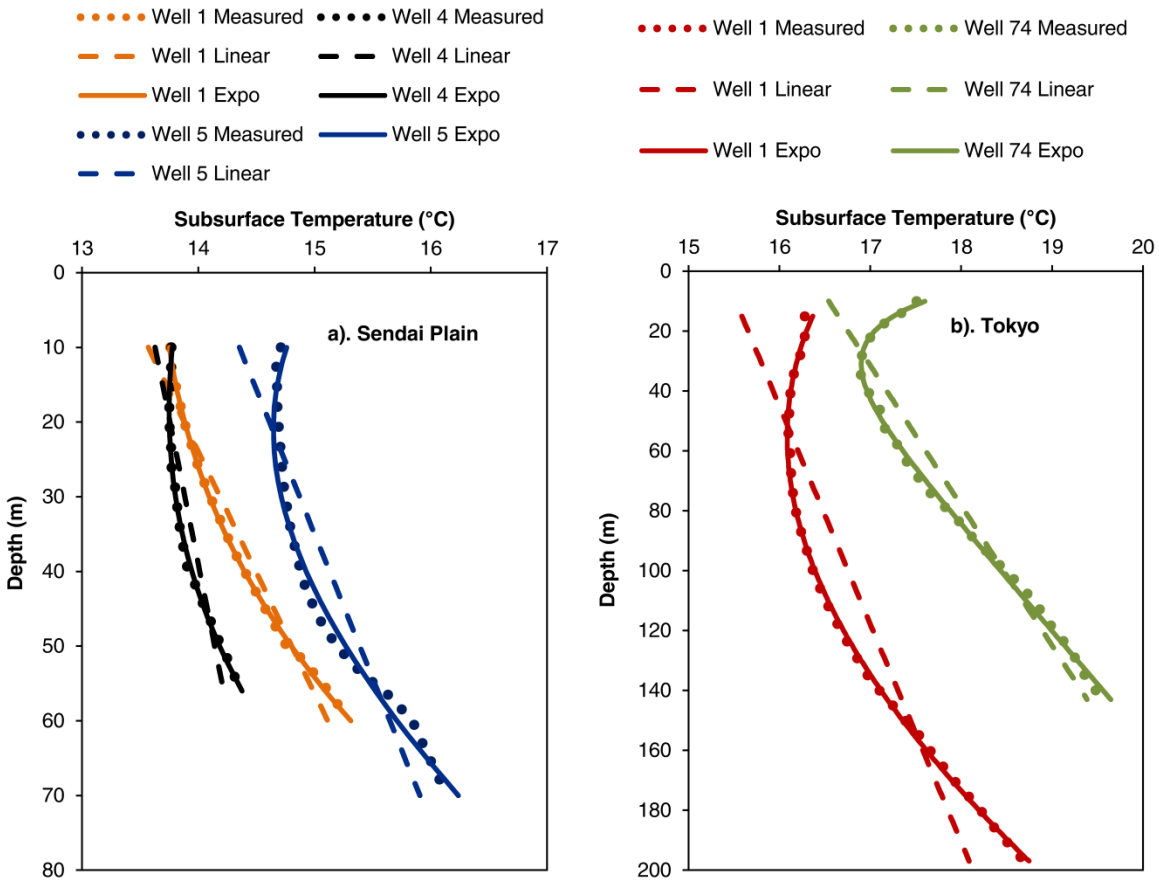

Figure 4: Measured borehole (BH) temperature data from (a) the Sendai Plain, Japan (data from Gunawardhana *et al.*, 2011) and (b) Tokyo, Japan (data from Taniguchi *et al.*, 1999). The associated linear (initial and boundary conditions, equation 2) and exponential (expo, equation 4) best fits for each BH are indicated by the dashed and continuous lines, respectively.

3.3. Results for illustrative examples with future surface warming

Temperature-depth profiles were generated from equation (8) for hypothetical surface warming and groundwater flow scenarios having the thermal properties, initial conditions, and boundary conditions described below. These simulations were also simulated with the SUTRA numerical code and thus served as verification problems. The thermal properties were obtained from Bonan (2008) and Oke (1978). The values assumed for the thermal conductivity of the medium λ, volumetric heat capacity of the medium $c\rho$, and heat capacity of water $c_w\rho_w$ were 2.20 $W \cdot m^{-1} \cdot °C^{-1}$, 2.96×10^6 $J \cdot m^{-3} \cdot °C^{-1}$, and 4.18×10^6 $J \cdot m^{-3} \cdot °C^{-1}$, respectively. These yield an effective heat diffusivity D for the medium of 7.43×10^{-7} $m^2 \cdot s^{-1}$. An initial surface temperature of 14°C was assumed for the simulations; this is approximately the current average global surface air temperature (Jones *et al*., 1999). In all cases, the initial conditions (black series) were assumed to be concave upwards due to recent warming. A typical geothermal gradient a of 0.025 $°C \cdot m^{-1}$ was imposed below the near surface concavity (equation 4). The exponential boundary condition used to match the A2 projections (Figure 3) was applied for the surficial boundary condition, as the A2 projections are often considered to be the most realistic of the IPCC emission scenarios. In its upcoming Fifth Assessment Report, the IPCC is adopting 'representative concentration pathways' (RCP, van Vuuren *et al*., 2011); the most extreme of these RCPs generally predicts more extreme warming than the A2 emission scenario. The exponential curve fitted to the A2 projections was shifted upwards by 14°C to represent the actual surface temperature rather than the temperature anomalies. The intent of using globally averaged current and projected surface temperatures for the boundary condition is to simulate the subsurface response to climate change at a representative location.

The temperature-depth results given in Figure 5 show that the analytical results (equation 8) are in excellent agreement with the SUTRA simulations. It is quite clear that at this groundwater flux (0.5 $m \cdot yr^{-1}$, Figure 5a and 5b), advection is a significant heat transport mechanism. Figure 5a indicates that groundwater recharge could accelerate the transport of warming surface temperatures into the shallow subsurface. Additionally, Figure 5b demonstrates that groundwater flow in discharge regions could exacerbate the increase in subsurface temperature, because the subsurface is being warmed from above (climate change) and from below (advective heat transport from deeper geothermal regions). Thus, it appears that the direction of the groundwater velocity will play an important role in determining the subsurface thermal response to climate change. Simulations for other groundwater fluxes were performed, and our results generally concurred with those of Bodri and Cermak (2005) in that groundwater fluxes exceeding 0.03 $m \cdot yr^{-1}$ discernibly perturbed the temperature profiles from a purely conductive regime. The temperature-depth profiles in Figure 5c exhibit a typical conductive response to a surficial thermal perturbation (Carslaw and Jaeger, 1959; Taniguchi *et al*., 1999).

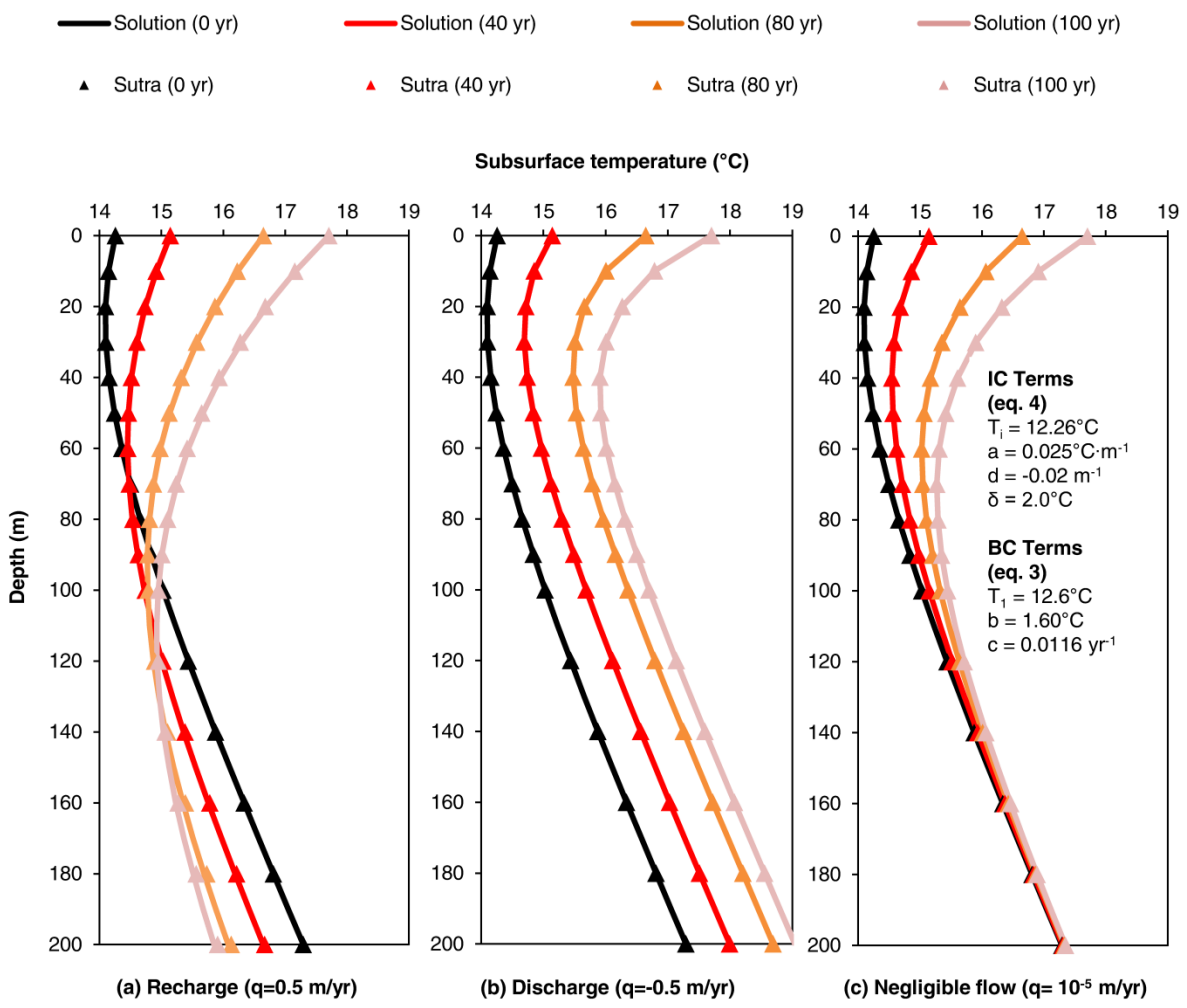

Figure 5: Temperature-depth profiles generated with Sutra and the analytical solution (equation 8) for the case of (a) recharge (downward flow), (b) discharge (upward flow), and (c) negligible flow. The equation parameters used to generate the initial conditions (IC) and boundary conditions (BC) are given in the inset. The thermal properties are provided in the text.

3.4. Comparison of equation (8) and the Taniguchi *et al*. (1999) solution

Previously compiled borehole data from the Sendai Plain were used to demonstrate the potential differences that may arise from the selection of the initial and boundary conditions (equation 8 vs. equation 2). These data were chosen as recent research has demonstrated that groundwater flow and heat transport in the Sendai Plain is primarily one-dimensional (Gunawardhana *et al*., 2011). The linear and exponential functions fitted to the temperature-depth profile in borehole 5 (Figure 4 and Table 1) were used as initial conditions for the simulations. Borehole 5 was chosen because it contained the deepest temperature profile. For both sets of initial conditions (i.e., linear and exponential), the initial surface

temperatures were found by extrapolating the curves up to the ground surface. The boundary conditions were then developed by adding the initial surface temperature to the exponential and linear A2 global surface temperature anomaly functions (Figure 3).

A vertical groundwater recharge flux of 0.130 $m \cdot yr^{-1}$ was imposed to match the value suggested by Gunawardhana *et al*. (Table 3, 2011). The thermal properties listed above were also utilized for these simulations. The analytical solution presented by Taniguchi *et al*. (1999) was applied to determine temperature-depth profiles for the case of linear initial conditions (from Borehole 5, Figure 4a, and Table 1) and a linear boundary condition. Equation (8) was used to determine temperature-depth profiles for the case of exponential initial and boundary conditions.

Figure 6 demonstrates the significant effect of the different initial conditions (black series) and boundary conditions. The initial condition has an inevitable impact on the boundary condition, because the two conditions (initial and boundary) are required to coincide at $t = 0$, $z = 0$. In this case, the solution of Taniguchi *et al*. (1999) underestimates shallow (upper 20 m) subsurface temperature on the order of 1°C and deeper (e.g., 100 m) subsurface temperature on the order of 2°C for 2100.

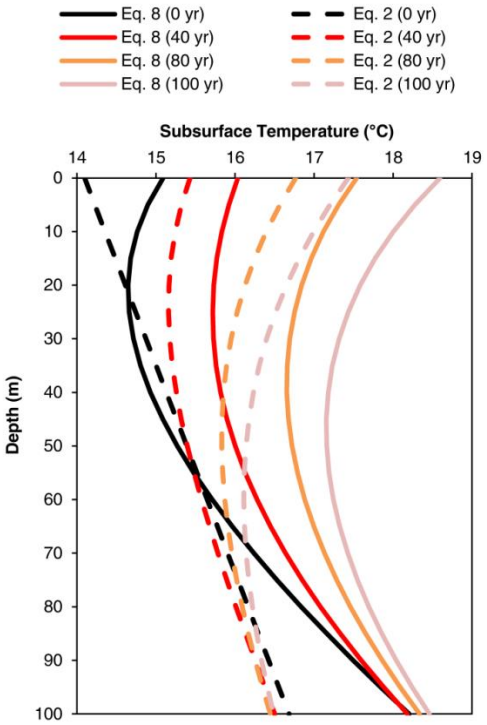

Figure 6: Temperature-depth profiles generated from equation (8) and the solution by Taniguchi *et al.* (1999) (equation 2) when the exponential and linear temperature profiles matched to Borehole 5 data (Figure 4a and Table 1) are used for initial conditions, and the surface is perturbed by the linear and exponential functions matched to the A2 global temperature anomaly projections (Figure 3).

4. Discussion

The preceding examples illustrated the application of the analytical solution to forward model the subsurface thermal impacts of climate change; however, the analytical solution can also be inverted to estimate past climate change trends from a borehole temperature profile. Other researchers have demonstrated the application of inverted forms of other analytical solutions to the conduction or conduction-advection equation to infer ground surface temperature history (e.g., Lachenbruch and Marshall, 1986; Beltrami *et al*., 1995; Taniguchi 2006). In this process, initial conditions are assumed for the temperature profile at some time before the present, and the boundary condition is adjusted until the simulated present-day temperature profile concurs with the measured profile. Various formal inversion techniques have been utilized to obtain the best fit between the simulated and measured borehole data (e.g., Mareschal and Beltrami, 1992, and references therein). These approaches have limitations because (1) the conduction-based solutions cannot be inverted to infer ground surface temperature in subsurface environments where advection is significant, and (2) the conduction-advection solution (i.e., equation 2) that has been inverted restricts the surface temperature history to a linear function.

The analytical solution proposed in equation (8) can be inverted without the two limitations noted above because it can accommodate groundwater flow and non-linear ground surface temperature changes. One question to be addressed in future research is how to establish the initial conditions for this inversion problem. Generally for inversion purposes, geothermal (i.e., linear) temperature profiles are assumed for initial conditions. Following the approach of others, the δ term in equation (4) can be set to zero to yield geothermal initial conditions for equation (8). However, even in the absence of climate change, the initial conditions may deviate from the geothermal profile if groundwater flow is significant. A potential solution to this problem is to generate appropriate initial conditions by first running the solution for a longer period (e.g., 10,000 years) with a constant boundary condition (b = 0 in equation 3) and the presumed groundwater flux. Equation (4) could then be fit to the results of such a simulation and used as the initial conditions for the inversion of a present-day borehole temperature profile. The formal inversion of this solution would not be onerous as the new boundary condition (equation 3) only contains one additional fitting parameter compared to the linear boundary condition of Taniguchi *et al*. (1999).

It should be noted that care must be employed when selecting an appropriate initial condition for the proposed solution for the purpose of forward modeling. If equation (4) is used to generate an initial condition by simply minimizing the RMSE between the function and measured borehole temperature data, very high temperatures may result at great depth, and these temperatures will eventually be conducted upwards. This effect will be exacerbated in regions of discharge, as advective heat flux will propagate the unreasonably high temperatures from below. It is recommended that the generated initial conditions be plotted

at depths much deeper than the region of interest to ensure that unreasonable results are not obtained. For this reason, results that extend far below measured borehole profiles should be considered with caution.

Finally, it should be recognized that the proposed analytical solution has inherent simplifications associated with the governing equation (e.g., one-dimensional water and heat flow, spatiotemporally constant groundwater velocity, no phase change in pore water, fully saturated conditions, and constant soil grain and soil water thermal properties). Additionally, the boundary condition cannot account for seasonal variations in temperature, and thus the shallow temperature-depth profiles produced by the solution represent annual average values.

5. Conclusions

An analytical solution for the one-dimensional conduction-advection equation was developed that can better accommodate measured temperature-depth profiles for initial conditions and air temperature projections for boundary conditions. For example, field data from the Sendai Plain and Tokyo, Japan were used to demonstrate the flexibility and improved accuracy of the initial conditions, and multi-model GCM air temperature projections from the IPCC were used to demonstrate the improved accuracy of the boundary condition. The solution was verified with numerical methods and applied to investigate the effect of surface warming and groundwater flow on hypothetical temperature-depth profiles. Results from these simulations indicated that groundwater recharge can exacerbate the rate of shallow subsurface warming, whereas groundwater discharge can transport heat from deeper geothermal zones.

To compare the differences between the analytical solution and the solution by Taniguchi *et al*. (1999), simulations were performed using the temperature profiles from the Sendai Plain, Japan as initial conditions and globally-averaged air temperature anomalies from the IPCC as the boundary condition. The results indicated that the differences between the two solutions can be significant (e.g., 1-2°C) in both the shallow and deeper subsurface thermal regimes. The potential of this solution to be applied to infer past ground surface temperate changes has also been discussed.

6. Acknowledgements

The comments from two anonymous reviewers and the Associate Editor significantly improved the quality of this paper. The climate projections produced by the IPCC are gratefully acknowledged. Luminda Gunawardhana of Tohoku University, Japan measured and provided the borehole temperature data beneath the Sendai Plain, Japan. Makoto Taniguchi of the Research Institute for Humanity and Nature, National Institute for Humanities, Japan generously provided the borehole temperature data for Tokyo, Japan.

References

Anderson M. 2005. Heat as a ground water tracer. *Ground Water* **43**: 951-68. DOI: 10.1111/j.1745-6584.2005.00052.x.

Andrushchyshyn O.P., Wilson K.P., Williams D.D. 2009. Climate change-predicted shifts in the temperature regime of shallow groundwater produce rapid responses in ciliate communities. *Global Change Biology* **15** : 2518-38. DOI: 10.1111/j.1365-2486.2009.01911.x.

Beltrami H., Chapman D., Archambault S., Bergeron Y. 1995. Reconstruction of high resolution ground temperature histories combining dendrochronological and geothermal data. *Earth and Planetary Science Letters* **136** : 437-45. DOI: 10.1016/0012-821X(95)00172-9.

Beltrami H., Kellman L. 2003. An examination of short- and long-term air–ground temperature coupling. *Global and Planetary Change* **38** : 291-303. DOI: 10.1016/S0921-8181(03)00112-7.

Beltrami H., Ferguson G., Harris R.N. 2005. Long-term tracking of climate change by underground temperatures. *Geophysical Research Letters* **32** : L19707. DOI: 10.1029/2005GL023714.

Birch F. 1948. The effects of Pleistocene climatic variations upon geothermal gradients. *American Journal of Science* **246** : 729-60. DOI: 10.2475/ajs.246.12.729.

Bodri L., Cermak V. 2005. Borehole temperatures, climate change and the pre-observational surface air temperature mean: allowance for hydraulic conditions. *Global and Planetary Change* **45** : 265-76. DOI: 10.1016/j.gloplacha.2004.09.001.

Bonan G. 2008. *Ecological climatology*. Cambridge University Press: United Kingdom; 549.

Breau C., Cunjak R.A., Peake S.J. 2011. Behaviour during elevated water temperatures: can physiology explain movement of juvenile Atlantic salmon to cool water? *Journal of Animal Ecology* **80** : 844-53. DOI: 10.1111/j.1365-2656.2011.01828.x.

Caissie D. 2006. The thermal regime of rivers: a review. *Freshwater Biology* **51** : 1389-406. DOI: 10.1111/j.1365-2427.2006.01597.x.

Carslaw H.S., Jaeger J.C. 1959. *Conduction of heat in solids*. Clarendon Press: Oxford; 520.

Crank J. 1980. *The mathematics of diffusion*. Clarendon Press: USA; 424.

Cunjak R., Roussel J.M., Gray M., Dietrich J., Cartwright D., Munkittrick K., Jardine T. 2005. Using stable isotope analysis with telemetry or mark-recapture data to identify fish movement and foraging. *Oecologia* **144** : 636-46. DOI: 10.1007/s00442-005-0101-9.

Farlow S.J. 1982. *Partial differential equations for scientists and engineers*. Wiley: New York; 388.

Ferguson G. 2007. Heterogeneity and thermal modeling of ground water. *Ground Water* **45** : 485-90. DOI: 10.1111/j.1745-6584.2007.00323.x.

Ferguson G., Woodbury A.D. 2004. Subsurface heat flow in an urban environment. *Journal of Geophysical Research-Solid Earth* **109** : B02402. DOI: 10.1029/2003JB002715.

Ferguson G., Woodbury A.D. 2005. The effects of climatic variability on estimates of recharge from temperature profiles. *Ground Water* **43** : 837-42. DOI: 10.1111/j.1745-6584.2005.00088.x.

Ferguson G., Beltrami H., Woodbury A.D. 2006. Perturbation of ground surface temperature reconstructions by groundwater flow? *Geophysical Research Letters* **33** : L13708. DOI: 10.1029/2006GL026634.

Ferguson G., Woodbury A.D. 2007. Urban heat island in the subsurface. *Geophysical Research Letters* **34** : L23713. DOI: 10.1029/2007GL032324.

González-Rouco J.F., Beltrami H., Zorita E., von Storch H. 2006. Simulation and inversion of borehole temperature profiles in surrogate climates: Spatial distribution and surface coupling. *Geophysical Research Letters* **33** : L01703. DOI: 10.1029/2005GL024693.

Green T.R., Taniguchi M., Kooi H., Gurdak J.J., Allen D.M., Hiscock K.M., Treidel H., Aureli A. 2011. Beneath the surface of global change: Impacts of climate change on groundwater. *Journal of Hydrology* **405** : 532-60. DOI: 10.1016/j.jhydrol.2011.05.002.

Gunawardhana L.N., Kazama S. 2011. Climate change impacts on groundwater temperature change in the Sendai plain, Japan. *Hydrological Processes* **25** : 2665-78. DOI: 10.1002/hyp.8008.

Gunawardhana L.N., Kazama S., Kawagoe S. 2011. Impact of urbanization and climate change on aquifer thermal regimes. *Water Resources Management* **25** : 3247-76. DOI: 10.1007/s11269-011-9854-6.

Harris R.N., Chapman D.S. 1997. Borehole temperatures and a baseline for 20th-century global warming estimates. *Science* **275** : 1618-21. DOI: 10.1126/science.275.5306.1618.

Hayashi M., Rosenberry D.O. 2002. Effects of ground water exchange on the hydrology and ecology of surface water. *Ground Water* **40** : 309-16. DOI: 10.1111/j.1745-6584.2002.tb02659.x.

Hinkel K.M., Outcalt K.M. 1993. Detection of nonconductive heat transport in soils using spectral analysis. *Water Resources Research* **29** : 1017-23. DOI: 10.1029/92WR02596.

IPCC. 2007. Intergovernmental Panel on Climate Change AR4 multi-model average of detrended globally averaged TAS anomalies. Available at: http://www.ipcc-data.org/data/ar4_multimodel_globalmean_tas.txt. Accessed, **2012**.

Javandel I., Doughty C., Tsang C. 1984. *Groundwater transport: handbook of mathematical models*. American Geophysical Union: Washington, D.C.; 94.

Jones P.D., New M., Parker D.E., Martin S., Rigor I.G. 1999. Surface air temperature and its changes over the past 150 years *Reviews of Geophysics* **37** : 173-99. DOI: 10.1029/1999RG900002.

Kane D.L., Hinkel K.M., Goering D.J., Hinzman L.D., Outcalt S.I. 2001. Non-conductive heat transfer associated with frozen soils. *Global and Planetary Change* **29** : 275-92. DOI: 10.1016/S0921-8181(01)00095-9.

Kukkonen I.T., Cermák V., Safanda J. 1994. Subsurface temperature-depth profiles, anomalies due to climatic ground surface temperature changes or groundwater flow effects. *Global and Planetary Change* **9** : 221-32. DOI: 10.1016/0921-8181(94)90017-5.

Kumar R.R., Ramana D.V., Singh R.N. 2012. Modelling near subsurface temperature with mixed type boundary condition for transient air temperature and vertical groundwater flow. *Journal of Earth System Sciences* **121** : 1177-84. DOI: 10.1007/s12040-012-0220-8.

Kurylyk B.L., Bourque C.P.-., MacQuarrie K.T.M. 2013. Potential surface temperature and shallow groundwater temperature response to climate change: an example from a small forested catchment in east-central New Brunswick (Canada). *Hydrology and Earth System Sciences Discussions* **10** : 3283-326. DOI: 10.5194/hessd-10-1-2013.

Lachenbruch A.H., Marshall B.V. 1986. Changing climate - Geothermal evidence from permafrost in the Alaskan Arctic. *Science* **234** : 689-96. DOI: 10.1126/science.234.4777.689.

Lesperance M., Smerdon J.E., Beltrami H. 2010. Propagation of linear surface air temperature trends into the terrestrial subsurface *Journal of Geophysical Research-Atmospheres* **115** : D21115. DOI: 10.1029/2010JD014377.

Lewis T.J., Wang K. 1992. Influence of terrain on bedrock temperatures. *Global and Planetary Change* **98** : 87-100. DOI: 10.1016/0921-8181(92)90028-9.

Lunardini V.J. 1981. *Heat transfer in cold climates*. Van Nostrand Reinhold Co.: New York; 731.

Mann M., Schmidt G. 2003. Ground vs. surface air temperature trends: Implications for borehole surface temperature reconstructions. *Geophysical Research Letters* **30** : 1607. DOI: 10.1029/2003GL017170.

Mareschal J., Beltrami H. 1992. Evidences for recent warming from perturbed geothermal gradients: examples from eastern Canada. *Climate Dynamics* **6** : 135-43. DOI: 10.1007/BF00193525.

Mayer T.D. 2012. Controls of summer stream temperature in the Pacific Northwest. *Journal of Hydrology* **475** : 323-35. DOI: 10.1016/j.jhydrol.2012.10.012.

McKenzie J.M., Voss C.I. 2013. Permafrost thaw in a nested groundwater-flow system. *Hydrogeology Journal*, **Published Online**. DOI: 10.1007/s10040-012-0942-3.

Mellander P., Lofvenius M.O., Laudon H. 2007. Climate change impact on snow and soil temperature in boreal Scots pine stands. *Climatic Change* **89** : 179-93. DOI: 10.1007/s10584-007-9254-3

Miyakoshi A., Uchida Y., Sakura Y., Hayashi T. 2003. Distribution of subsurface temperature in the Kanto Plain, Japan; estimation of regional groundwater flow system and surface warming. *Physics and Chemistry of the Earth* **28** : 467-75. DOI: 10.1016/S1474-7065(03)00066-4.

Molina-Giraldo N., Bayer P., Blum P. 2011. Evaluating the influence of thermal dispersion on temperature plumes from geothermal systems using analytical solutions. *International Journal of Thermal Sciences* **50** : 1223-31. DOI: 10.1016/j.ijthermalsci.2011.02.004.

Ogata A., Banks R. 1961. A solution of the differential equation of longitudinal dispersion in porous media. **Professional Paper 411-A,** U.S. Geological Survey, Washington.

Oke T.R. 1978. *Boundary layer climates*. Methuen and Co.: London; 435.

Özışık M.N. 1968. *Boundary value problems of heat conduction*. International Textbook Co.: Scranton, PA; 505.

Pollack H.N., Huang S.P., Shen P.Y. 1998. Climate change record in subsurface temperatures: A global perspective. *Science* **282** : 279-81. DOI: 10.1126/science.282.5387.279.

Pollack H.N., Smerdon J.E., van Keken P.E. 2005. Variable seasonal coupling between air and ground temperatures: A simple representation in terms of subsurface thermal diffusivity. *Geophysical Research Letters* **32** : L15405. DOI: 10.1029/2005GL023869.

Qian B., Gregorich E.G., Gameda S., Hopkins D.W., Wang X.L. 2011. Observed soil temperature trends associated with climate change in Canada. *Journal of Geophysical Research-Atmospheres* **116** : 1-16. DOI: 10.1029/2010JD015012.

Reiter M. 2005. Possible ambiguities in subsurface temperature logs: Consideration of ground-water flow and ground surface temperature change. *Pure and Applied Geophysics* **162** : 343-55. DOI: 10.1007/s00024-004-2604-4.

Rike A.G., Schiewer S., Filler D.M. 2008. Temperature effects on biodegradation of petroleum contaminants in cold soils. . In *Bioremediation of petroleum hydrocarbons in cold regions*, Miller DM, Snape I, David L (eds). Cambridge University Press: Cambridge, UK; 84-108.

Roberts G.E., Kaufman H. 1966. *Table of Laplace transforms*. Saunders: Philadelphia.

Roy J.W., Zaitlin B., Hayashi M., Watson S.B. 2011. Influence of groundwater spring discharge on small-scale spatial variation of an alpine stream ecosystem. *Ecohydrology* **4** : 661-70. DOI: 10.1002/eco.156.

Saar M.O. 2011. Review: Geothermal heat as a tracer of large-scale groundwater flow and as a means to determine permeability fields. *Hydrogeology Journal* **19** : 31-52. DOI: 10.1007/s10040-010-0657-2.

Sauty J.P., Gringarten A.C., Menjoz A. 1982. Sensible energy storage in aquifers 1. Theoretical study. *Water Resources Research* **18** : 245-52. DOI: 10.1029/WR018i002p00245

Sharma L., Greskowiak J., Ray C., Eckert P., Prommer H. 2012. Elucidating temperature effects on seasonal variations of biogeochemical turnover rates during riverbank filtration. *Journal of Hydrology* **428** : 104-15. DOI: 10.1016/j.jhydrol.2012.01.028.

Smerdon J.E., Pollack H.N., Cermak V., Enz J.W., Kresl M., Safanda J., Wehmiller J.F. 2004. Air-ground temperature coupling and subsurface propagation of annual temperature signals. *Journal of Geophysical Research-Atmospheres* **109** : D21107. DOI: 10.1029/2004JD005056.

Smerdon J.E., Pollack H.N., Cermak V., Enz J.W., Kresl M., Safanda J., Wehmiller J.F. 2006. Daily, seasonal, and annual relationships between air and subsurface temperatures. *Journal of Geophysical Research-Atmospheres* **111** : D07101. DOI: 10.1029/2004JD005578.

Solomon S., Qin D., Manning M., Chen Z., Marquis M., Averyt K., Tignore M., Miller H.(eds). 2007. *Climate Change 2007: The Physical Science Basis. Contributions of Working Group I to the Fourth Assessment Report of the Intergovernmental Panel on Climate Change*. Cambridge University Press: Cambridge; 1056.

Stallman R.W. 1963. Computation of ground-water velocity from temperature data. In *Methods of Collecting and Interpreting Ground-Water Data: Water Supply Paper 1544-H*, Bentall R (ed). U.S. Geological Survey, Reston, Virginia; 35-46.

Stallman R.W. 1965. Steady one-dimensional fluid flow in a semi-infinite porous medium with sinusoidal surface temperature. *Journal of Geophysical Research* **70** : 2821-7. DOI: 10.1029/JZ070i012p02821.

Stieglitz M., Smerdon J.E. 2007. Characterizing land-atmosphere coupling and the implications for subsurface thermodynamics. *Journal of Climate* **20** : 21-37. DOI: 10.1175/JCLI3982.1.

Suzuki S. 1960. Percolation measurements based on heat flow through soil with special reference to paddy fields. *Journal of Geophysical Research* **65** : 2883-5. DOI: 10.1029/JZ065i009p02883.

Taniguchi M. 2006. Anthropogenic effects on subsurface temperature in Bangkok. *Climate of the Past Discussions* **2** : 831-46.

Taniguchi M., Shimada J., Uemura T. 2003. Transient effects of surface temperature and groundwater flow on subsurface temperature in Kumamoto Plain, Japan. *Physics and Chemistry of the Earth, Parts A/B/C* **28** : 477-86. DOI: 10.1016/S1474-7065(03)00067-6.

Taniguchi M., Shimada J., Tanaka T., Kayane I., Sakura Y., Shimano Y., Dapaah-Siakwan S., Kawashima S. 1999. Disturbances of temperature-depth profiles due to surface climate change and subsurface water flow: 1. An effect of linear increase in surface temperature caused by global warming and urbanization in the Tokyo Metropolitan Area, Japan. *Water Resources Research* **35** : 1507-17. DOI: 10.1029/1999WR900009.

Taniguchi M., Shimada J., Fukuda Y., Yamano M., Onodera S., Kaneko S., Yoshikoshi A. 2009. Anthropogenic effects on the subsurface thermal and groundwater environments in Osaka, Japan and Bangkok, Thailand. *Science of The Total Environment* **407** : 3153-64. DOI: 10.1016/j.scitotenv.2008.06.064.

Taniguchi M., Uemura T. 2005. Effects of urbanization and groundwater flow on the subsurface temperature in Osaka, Japan. *Physics of the Earth and Planetary Interiors* **152** : 305-13. DOI: 10.1016/j.pepi.2005.04.006.

Taylor C.A., Stefan H.G. 2009. Shallow groundwater temperature response to climate change and urbanization. *Journal of Hydrology* **375** : 601-12. DOI: 10.1016/j.jhydrol.2009.07.009.

Torgersen C.E., Ebersole J.L., Keenan D.M. 2012. Primer for identifying cold-water refuges to protect and restore thermal diversity in riverine landscapes. **EPA 910-C-12-001**, U.S. Environmental Protection Agency, Seattle, Washington. Available at: http://www.epa.gov/region10/pdf/water/torgersen_etal_2012_cold_water_refuges.pdf

Trim D.W. 1990. *Applied partial differential equations*. PWS-KENT Publishing Company: Boston, MA; 483.

Uchida Y., Hayashi T. 2005. Effects of hydrogeological and climate change on the subsurface thermal regime in the Sendai Plain. *Physics of the Earth and Planetary Interiors* **152** : 292-304. DOI: 10.1016/j.pepi.2005.04.008.

Uchida Y., Sakura Y., Taniguchi M. 2003. Shallow subsurface thermal regimes in major plains in Japan with reference to recent surface warming. *Physics and Chemistry of the Earth, Parts A/B/C* **28** : 457-66. DOI: 10.1016/S1474-7065(03)00065-2.

van der Kamp G., Bachu S. 1989. Use of dimensional analysis in the study of thermal effects of various hydrogeological regimes. In *Hydrogeological regimes and their subsurface thermal effects, Geophysical Monograph 47*, Beck AE, Garven G, Stegena L (eds). American Geophysical Union: Washington DC; 23-28.

van Vuuren D.P., Edmonds J., Kainuma M., Riahi K., Thomson A., Hibbard K., Hurtt G.C., Kram T., Krey V., Lamarque J., Masui T., Meinshausen M., Nakicenovic N., Smith S.J., Rose S.K. 2011. The representative concentration pathways: an overview. *Climatic Change* **109** : 5-31. DOI: 10.1007/s10584-011-0148-z.

Voss C.I., Provost A.M. 2010. SUTRA: A model for saturated-unsaturated variable-density ground-water flow with solute or energy transport. **Water Resources Investigations Report 02-4231** : U.S. Geological Survey, Reston, Virgina; 260.

Warrick A.W. 2003. *Soil water dynamics*. Oxford University Press: New York, New York; 391.

Webb B.W., Hannah D.M., Moore R.D., Brown L.E., Nobilis F. 2008. Recent advances in stream and river temperature research. *Hydrological Processes* **22** : 902-18. DOI: 10.1002/hyp.6994.

Williams P.J., Smith M.W. 1989. *The frozen earth: Fundamentals of geocryology*. Cambridge University Press: Cambridge; New York; 306.

Woodbury A.D., Smith L. 1985. On the thermal effects of three-dimensional groundwater flow. *Journal of Geophysical Research* **90** : 759-67. DOI: 10.1029/JB090iB01p00759.

Zhang T.J. 2005. Influence of the seasonal snow cover on the ground thermal regime: An overview. *Reviews of Geophysics* **43** : RG4002. DOI: 10.1029/2004RG000157.

Zill D.G. 2005. *A first course in differential equations with modeling applications*. Brooks/Cole: Belmont, CA; 393.